

# Geohistory Analysis and Petroleum Reservoir Characteristics of Lower Cretaceous (Neocomian) Sandstones, Eastern Kopet-Dagh Basin, Northeastern Iran<sup>1</sup>

Reza Moussavi-Harami<sup>2</sup> and Robert L. Brenner<sup>3</sup>

## ABSTRACT

The eastern part of the Kopet-Dagh basin of northeastern Iran contains over 4000 m of Upper Jurassic through Tertiary strata deposited in a variety of shallow-marine and terrestrial environments. Geohistory diagrams from well and outcrop data provide a useful mechanism with which to relate the stratigraphic framework of this part of the basin to the tectonic history of the region. During some episodes of regional tectonic uplift (e.g., episodes occurring 99–95 Ma, 74–70 Ma, and 63–54 Ma), sediment accommodation space continued to be created in the basin due to sediment loading and compaction of increased amounts of fine-grained sediments, in some cases concomitant with eustatic sea level rises. Much of the post-Jurassic subsidence in this part of the Kopet-Dagh basin was caused by sediment loading rather than tectonism.

The effects of basin geohistory on petroleum reservoir properties were studied using the Lower Cretaceous (Neocomian) Shurijeh Formation as an example. Detailed petrologic, sedimentologic, and geohistory analyses done on this formation show that the petroleum reservoir properties of Shurijeh sandstones were affected by their depositional settings and the

subsequent subsidence of these units through meteoric and compactional hydrogeologic regimes in this part of the Kopet-Dagh basin. These rocks consist mostly of sublitharenitic red beds deposited during a regressive phase of sedimentation dominated by rapid siliciclastic sediment supply. The lower and middle parts of the interval studied were deposited in low-sinuosity braided fluvial systems, and the upper part was deposited in high-sinuosity meandering systems. By relating the paragenetic sequence of the Shurijeh sandstones to the geohistory of this formation, we determined the timing of both porosity-destroying and porosity-enhancing diagenetic processes and related these processes to the timing of petroleum generation.

## INTRODUCTION

The Kopet-Dagh basin of northeastern Iran was formed during the early Mesozoic. Jurassic through Tertiary rocks crop out within an eastward-plunging anticline in the eastern part of the basin (Figure 1). The geohistory analysis presented in this paper is based on data collected from three gas wells (KG-2 in the Khangiran gas field, and GL-2 and GL-3 in the Gonbadli gas field) that produce from Upper Jurassic carbonates and Lower Cretaceous red beds, and from observations along the outcrop belt south of these wells (Figure 1).

Our study was designed to integrate tectonic, stratigraphic, and petrographic information generated from this part of the Kopet-Dagh basin (e.g., Afshar-Harb, 1969, 1979, 1982; Kalantari, 1969, 1987; Moussavi-Harami, 1986, 1989, 1990; Moussavi-Harami and Brenner, 1990 and unpublished data). In this paper, we discuss the construction and interpretations of geohistory diagrams for the eastern part of the Kopet-Dagh basin, summarize the depositional and diagenetic history of the Lower Cretaceous (Neocomian) Shurijeh Formation, and relate the diagenetic history of this petroleum-bearing unit to the geohistory of this basin.

©Copyright 1992. The American Association of Petroleum Geologists. All rights reserved.

<sup>1</sup>Manuscript received June 26, 1991; revised manuscript received February 5, 1992; final acceptance March 2, 1992.

<sup>2</sup>Department of Geology, Faculty of Science, Mashhad University, Mashhad, Iran 91384.

<sup>3</sup>Department of Geology, University of Iowa, Iowa City, Iowa 52242.

The University of Mashhad provided financial support for Moussavi-Harami while he served as a visiting professor of geology at the University of Iowa. Computing and other facilities were provided by the Department of Geology at the University of Iowa. Core samples, thin sections of outcrop samples, well logs, and logistical support for Moussavi-Harami were supplied by the Exploration and Production Group of the National Iranian Oil Company. Thin sections of core samples were made by Kay Saville at the University of Iowa. Critical reviews of various versions of this manuscript were provided by Philip H. Heckel, Greg A. Ludvigson, Frank G. Ethridge, Kinji Magara, Donald Nelson, and an anonymous reviewer.

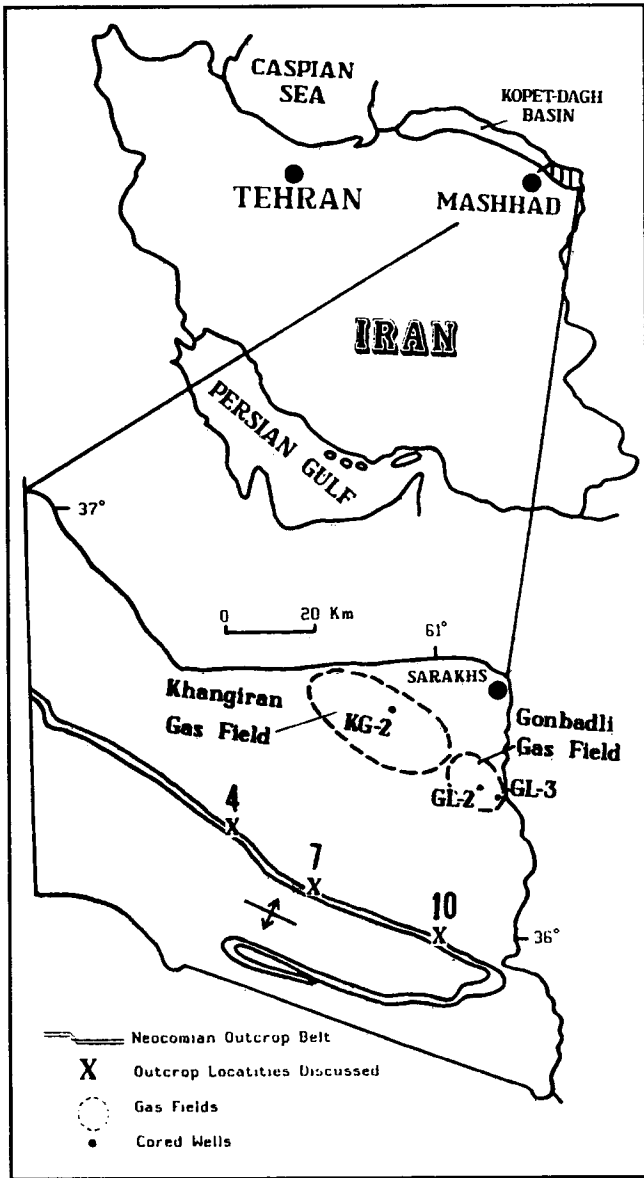


Figure 1—Index and general geologic map of eastern part of Kopet-Dagh basin (modified from Huber, 1975) showing locations of gas fields and wells where data were collected.

**REGIONAL GEOLOGIC SETTING**

The Kopet-Dagh formed as an intracontinental basin in northern Iran after closure of the Hercynian Ocean following the Middle Triassic (early Kimmerian) orogeny (Berberian and King, 1981). From the Jurassic through the Eocene, relatively continuous sedimentation, recorded by five major transgressive-regressive sequences, took place in the eastern Kopet-Dagh basin (Figure 2) (Afshar-Harb, 1969, 1979, 1982; Kalantari, 1987). During the Early Jurassic, the sea transgressed to

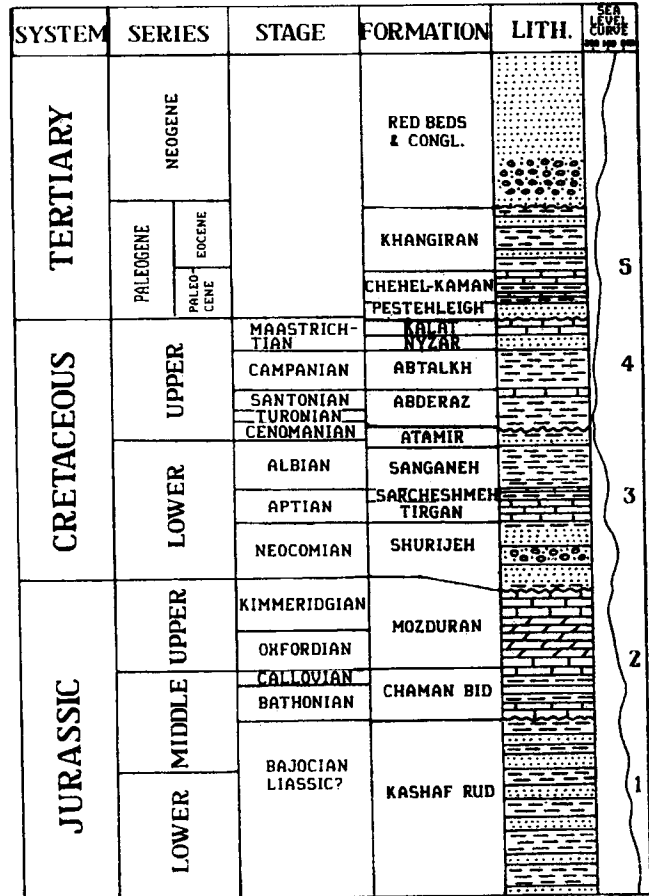


Figure 2—Generalized stratigraphic chart for the eastern Kopet-Dagh basin and global eustatic sea level curve modified from Haq et al. (1987). Standard lithologic symbols used in lithology column (dots and circles for sandstones and conglomerates, dashes for siliciclastic mudrocks, rectangles for limestone, parallelograms for dolomite, and wavy lines for unconformities). Numbers 1–5 in the sea level column refer to informal sequences mentioned in text.

the southeast and a thick interval of siliciclastic sediments was deposited as deltaic and marine sedimentary complexes (sequence 1 on Figure 2) (Madani, 1977). During the Late Jurassic, the easternmost part of the basin received siliciclastic sediments while the remainder of the study area received marine carbonate sediments (sequence 2 on Figure 2).

From near the end of the Jurassic through the Early Cretaceous (Neocomian), the sea withdrew from the eastern Kopet-Dagh basin toward the northwest, and a 230- to 900-m-thick interval of fluvial siliciclastic sediments was deposited across the eastern part of the basin (Moussavi-Harami, 1986; Moussavi-Harami and Brenner, 1990). The marine limestones west of the study area record the establishment of marine environ-

ments sometime during the Early Cretaceous in the central and western parts of the Kopet-Dagh basin (sequence 3 on Figure 2) (Kalantari, 1969; Afshar-Harb, 1979). Later, southeastward transgressions across the Sarakhs area established marine environments that persisted through the Late Cretaceous, except for a short period during the Turonian (sequence 4 on Figure 2). Red beds of the Pestehleigh Formation were deposited during the early Paleocene regression and were followed by deposition of marine and nonmarine Paleocene and Eocene sediments (sequence 5 on Figure 2). Repeated transgressions and regressions continued through the Miocene, when the basin was folded during the late Alpine compression, creating the anticlinal traps of the Khangiran and Gonbadli gas fields.

## GEOHISTORY

### Construction of Geohistory Diagrams

The geohistory diagrams for the eastern Kopet-Dagh basin were constructed for the KG-2, GL-2, and GL-3 wells, starting at the base of the Upper Jurassic Mozduran Formation. Ages used for Figures 3 and 5 were determined by calibrating the biostratigraphic work of Kalantari (1969, 1987) to the global correlations, and were compared to the sea level chronology suggested by Haq et al. (1987). We used computation procedures of Van Hinte (1978), Sclater and Christie (1980), and Angevine et al. (1990) involving the following sediment compaction equations to calculate decompacted sediment thicknesses.

$$\phi_n = \phi_o \exp(-cz) \quad (1)$$

where  $\phi_n$  = porosity of the unit,  $\phi_o$  = original porosity,  $c$  = constant for each lithology, and  $z$  = present depth.

$$T_o = \frac{(1 - \phi_n)T_n}{1 - \phi_o} \quad (2)$$

where  $T_o$  = original thickness,  $\phi_n$  = porosity of the unit,  $\phi_o$  = original porosity, and  $T_n$  = present-day thickness.

We used the local isostatic balance method to compute tectonic subsidence because we could assign realistic values to required parameters (Table 1). Our current state of knowledge about crustal conditions in the Kopet-Dagh area is inadequate to confidently assign values to parameters used in the more realistic regional flexural analysis method described by Angevine et al. (1990). The following two equations were used to compute tectonic subsidence.

$$\rho_s = \frac{\sum_i [\phi_i \rho_w + (1 - \phi_i) \rho_g] T_i}{S} \quad (3)$$

**Table 1. Geologic Parameters Used in Preparation of Geohistory Diagrams**

Component	Original Porosity (%)	$c^*$	Density
Sandstone	45	$3 \times 10^{-4}$	2.65
Shaly Sandstone, Silty Shale	50	$4 \times 10^{-4}$	2.65
Marlstone, Chalky Limestone, & Clay Shale	60	$5 \times 10^{-4}$	2.65
Limestone & Dolostone	50	$7 \times 10^{-4}$	2.71
Water	—	—	1.03
Asthenosphere	—	—	3.3

\* $c$  = compaction constant for each lithology.

where  $\rho_s$  = density of sediment,  $\phi_i$  = porosity of unit,  $\rho_w$  = density of water (for subaerial depositional environment,  $\rho_w = 0$ ),  $\rho_g$  = grain density (not the same as sediment density),  $T_i$  = thickness of the unit,  $S$  = thickness of uncompacted sediment column.

$$Z_i = S \left[ \frac{(\rho_a - \rho_s)}{(\rho_a - \rho_w)} \right] + Wd_i \quad (4)$$

where  $S$  = thickness of uncompacted sediment column,  $Z_i$  = amount of tectonic subsidence,  $\rho_a$  = density of the asthenosphere,  $\rho_s$  = density of sediment,  $\rho_w$  = density of water, and  $Wd_i$  = depth of water for unit  $i$ .

Densities ( $\rho$ ), porosities ( $\phi$ ), and lithology constants ( $c$ ) that we used in these calculations are shown in Table 1. Rock types and thicknesses for each stratigraphic interval were determined from analyses of rock exposures, core materials, well logs, driller's logs, and from published regional stratigraphic studies (e.g., Afshar-Harb, 1969, 1979, 1982; Kalantari, 1969, 1987). Porosity measurements and density values were selected from the middle of each stratigraphic unit shown on Figure 2. Water depths were estimated from paleontological data (Kalantari, 1969, 1987) and by comparing lithofacies with analogous present-day environments. Because the Kopet-Dagh basin was an intracontinental basin for most of its history, we assumed that maximum water depths did not exceed 200 m. This assumption is consistent with Mesozoic and Cenozoic lithofacies and biofacies studied in this part of the basin, and is within eustatic sea level fluctuations of about 150 m suggested by Haq et al. (1987). Assuming that these water depth constraints are at least approximately correct, then Late Jurassic to present-day paleobathymetry variations would not be apparent on the scale that we used in the construction of our geohistory diagrams.

### Implications From Diagrams

The results of this geohistory analysis are illustrated by diagrams constructed from well GL-3 (Figure 3A, B);

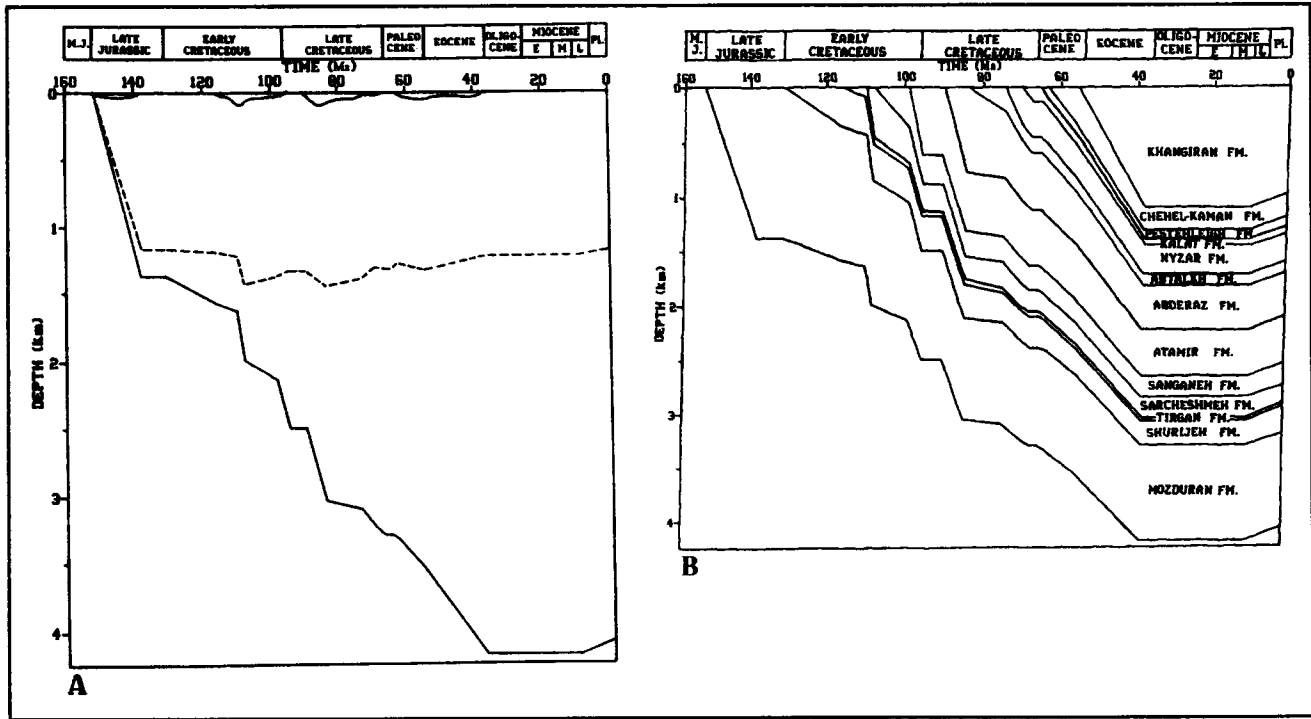


Figure 3—Geohistory diagrams for well GL-3. (A) Total subsidence (solid line) and tectonic subsidence and uplift (dashed line) for the base of the Upper Jurassic Mozduran Formation. (B) Total subsidence for the base of each stratigraphic unit between the Upper Jurassic and Neogene.

these diagrams are similar to those from wells KG-2 and GL-2. The base of Upper Jurassic sedimentary strata subsided at a relatively high rate through the Late Cretaceous (Figure 3A). Total subsidence was a result of relatively high rates of tectonic subsidence (152 Ma and 84 Ma) during early stages of basin formation, coupled with high sediment supply rates that continued until about 37 Ma (Figure 3B). The subsidence rate decreased as the rates of sediment supply to the basin decreased in the Oligocene. The late Alpine Orogeny began about 10 Ma, and was recorded in the Kopet-Dagh basin by uplifting of previously deposited strata (Figure 3A).

During the Late Jurassic, sediments in the eastern Kopet-Dagh basin subsided at a relatively high average (calculated) rate of 98.2 m per m.y. This high subsidence rate, coupled with the dominance of carbonates over siliciclastics (Mozduran Formation, Figures 2, 3B), are compatible with the concept that tensional tectonic subsidence was greatest at the beginning of Kopet-Dagh basin formation. Similar rapid subsidence existed in the western part of the basin where Afshar-Harb (1979) reported that four longitudinal faults, active since the Jurassic, caused the Kopet-Dagh to have subsided more rapidly than the block to the south. This period of subsidence was followed by a period of uplift

and erosion in the western part of the basin during the Early Cretaceous. In the southern part of the study area, the outcrop belt shows Lower Cretaceous red beds resting disconformably above Lower–Middle Jurassic rocks (Kashaf Rud Formation, sequence 1-2 boundary on Figure 2) (Moussavi-Harami, 1990), with the intervening carbonates removed by erosion. This period of uplift and erosion marked a change in sedimentary style, from carbonate dominance to siliciclastic dominance, that lasted through much of the Neocomian (sequence 3 on Figure 2; Figure 3B).

During the late Aptian, the Kopet-Dagh basin subsided abruptly and relatively deep-water (approximately 100–150 m) marlstones were deposited across the study area, followed by a relative sea level fall and deposition of shallow-water siliciclastic sediments during the Albian and early Cenomanian. Late in the Cenomanian, epeirogenic activity began in the western part of the basin, causing a period of nondeposition and possibly erosion. In the eastern Kopet-Dagh basin, epeirogeny resulted in a disconformity between Cenomanian and Turonian rocks. This disconformity has been demonstrated paleontologically (sequence 3–4 boundary on Figure 2) (Kalantari, 1969). Orogenic activity was much greater in the western part of the basin, where an angular unconformity between the

Cenomanian and Maastrichtian sediments was observed (Afshar-Harb, 1979). In the study area, epeirogeny is recorded on the geohistory diagrams as an trending-upward segment on the tectonic subsidence curve between 99 and 95 Ma, but the total subsidence curve shows a continued downward-trending segment for the same time interval due to sediment loading effects (Figure 3A). The time of nondeposition (95–90 Ma) is represented on both curves as horizontal segments. The same subsidence curve characteristics are found on the geohistory diagrams for the KG-2 and GL-2 wells. We interpret this apparent inconsistency during the 95–90 Ma interval to be due to sediment loading and compaction resulting from continued high rates of fine-grained siliciclastic deposition prior to and during the period of regional uplift. Nondeposition in this area during this 95–90 Ma interval resulted from elimination of accommodation space by a combination of high sedimentation rates and sea level fall.

In the eastern Kopet-Dagh basin, the subsidence rate again increased to approximately 96 m per m.y. as a result of both tectonic and sediment loading during the late Turonian through the Santonian (Figure 3A). Uplifting resumed about 74 Ma, but subsidence continued due to sediment loading and an apparent rise in eustatic sea level (according to curves published by Haq et al., 1987) that allowed an increase in accommodation space. As a result, a very shallow-marine environment was established during the early Maastrichtian, and was maintained through the middle Maastrichtian in the study area. The middle Alpine orogeny, which started during the middle Maastrichtian, initiated withdrawal of the Kopet-Dagh seaway from the study area. As a result, lower Paleocene red beds were deposited disconformably above very shallow-marine Upper Cretaceous sediments (sequence 4–5 boundary on Figure 2). These events are depicted on Figure 3A by trending-upward segments on the tectonic subsidence curve (65–63 Ma) and concomitant trending-downward segments on the total subsidence curve. As was the case in the Cenomanian, sediment influx caused continued subsidence because the effect of sediment loading and compaction were great enough to overcome the epeirogenic tectonic movements in the region.

Another episode of tectonic uplift coupled with sediment loading and continued total subsidence took place from the early to late Paleocene (63–54 Ma) in the study area (Figure 3A). During this time, sea level rose at a high enough rate to abruptly shift potential siliciclastic point sources far from this part of the basin, allowing the carbonates of the Chehel-Kaman Formation to be deposited (Figure 2). From very late Paleocene to late Eocene (54–37 Ma), relative sea level dropped and very shallow-marine to shoreline siliciclastic sediments were deposited in the last phase of marine sedimentation in the eastern Kopet-Dagh basin (sequence 5 on Figure 2). Along the outcrop belt, non-marine red beds lie disconformably above Eocene

shoreline sediments (Figure 2), indicating that Kopet-Dagh sedimentation was dominantly nonmarine during the Neogene. These rocks are not present in the wells from which our geohistory diagrams were constructed due to nondeposition and erosion in the northern part of the study area. The period between 37 and 10 Ma is depicted on our geohistory diagrams as horizontal line segments, indicating that nondeposition and erosion took place. During the late Alpine orogeny (about 10 Ma), the basin was uplifted and deformed (trending-upward line segments between 10–0 Ma on Figure 3), resulting in the formation of anticlines and synclines, some of which formed hydrocarbon traps.

An important implication derived from these geohistory diagrams is that from the late Aptian through the late Eocene, subsidence in this part of the Kopet-Dagh basin was due predominantly to sediment loading rather than tectonic factors because highly compressible muds comprised approximately 73% of this part of the stratigraphic section. Sediment compaction created additional accommodation space, allowing more sediments to accumulate and adding to the sediment loading effect. Although the wells used in this study do not penetrate deep enough to show the hydrocarbon-generating window for this part of the basin, similarly constructed diagrams can be used as guides for determining total subsidence and predicting the depths to hydrocarbon-generation windows in places where well penetrations reach these windows.

#### **AFFECT OF KOPET-DAGH GEOHISTORY ON LOWER CRETACEOUS (SHURIJEH FORMATION) SANDSTONE RESERVOIRS**

##### **Neocomian Depositional Environments and Paleogeography**

During the Late Jurassic–Early Cretaceous regression toward the northwest, continental sedimentation was established in the eastern part of the Kopet-Dagh basin. Along the outcrop belt in the western part of the study area, limestone pebbles containing Upper Jurassic fossils are included in Lower Cretaceous conglomerates, indicating that nearby Upper Jurassic carbonates were eroded during the Early Cretaceous. In addition, metamorphic lithic pebbles that petrographically match Jurassic metamorphic complexes southwest of the study area are most abundant in the south and southwestern parts of the study area, decreasing in abundance northward (Moussavi-Harami and Brenner, 1990). Lithologic and textural characteristics, paleocurrent analysis, along with lateral and vertical facies relationships studied along the outcrop belt, indicate that the red bed siliciclastics of the Shurijeh Formation were derived from metamorphic and sedimentary source areas to the southwest and deposited in fluvial environments (Moussavi-Harami and Brenner, 1990).

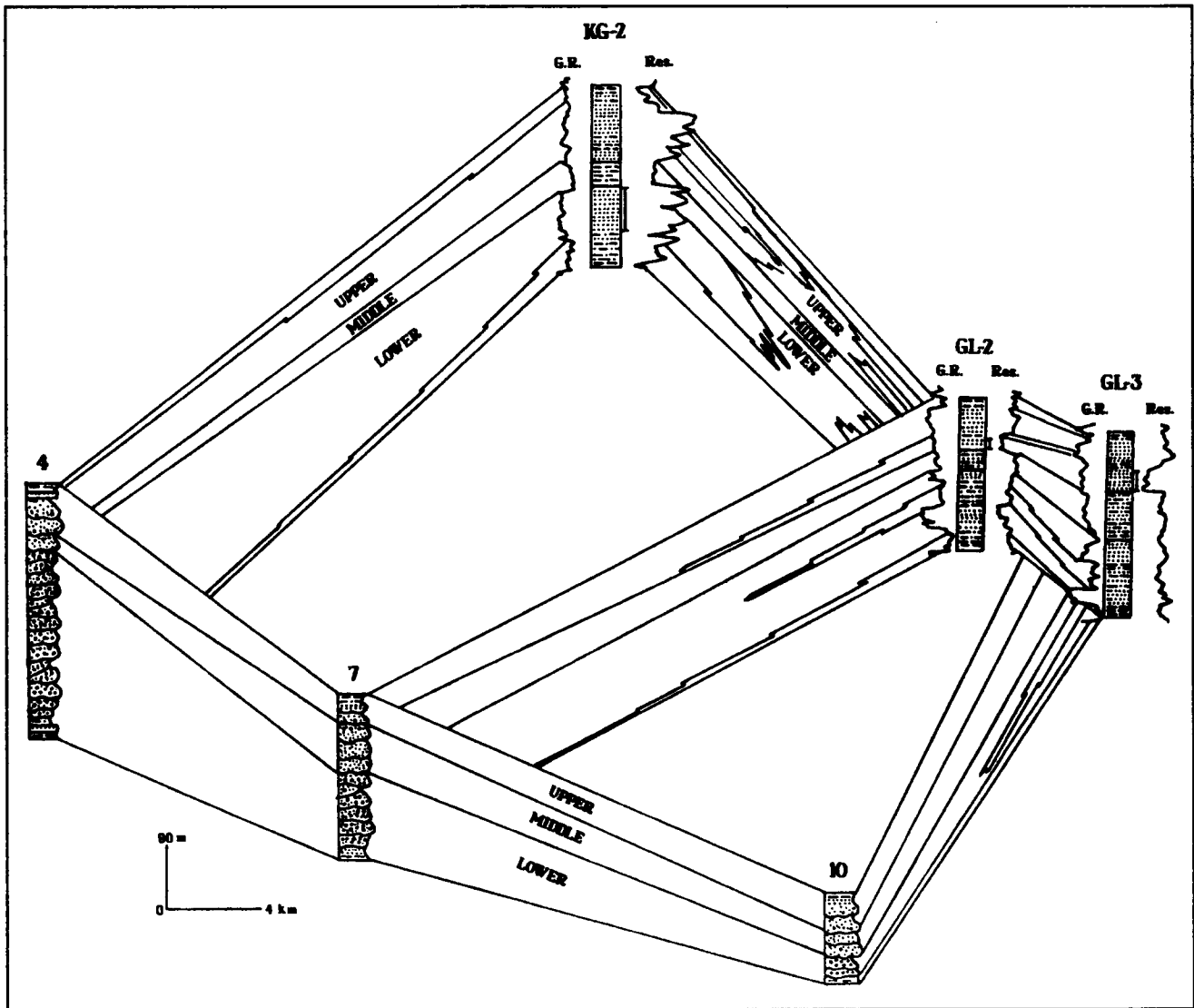


**Figure 4**—Fence diagram showing stratigraphic and lithofacies relationships in the Shurijeh Formation between the outcrop belt (measured sections 4, 7, and 10) and subsurface in the Sarakhs area (wells KG-2, GL-2, and GL-3). See Figure 1 for locations. Vertical bars next to stratigraphic columns show reservoir intervals.

A sedimentologic study of the Shurijeh Formation along its outcrop belt shows that these rocks were deposited in three distinct parts (Figure 4) (Moussavi-Harami and Brenner, 1990). The lowest part of the interval is characterized by a dominance of blocky cross-bedded and homogenous conglomerates, with a lesser amount of cross-bedded pebbly sandstones, and minor mudstone strata. The middle part of the interval consists of fine- to coarse-grained cross-bedded and parallel-laminated pebbly sandstone with minor mudstone strata. Sandstones in this part of the section form sheet-like bodies that were traced laterally for many kilometers along the outcrop belt. The upper part of the interval consists of fining-upward sequences of

conglomerate and sandstone separated by strata of silty and clayey shale.

Moussavi-Harami and Brenner (1990) interpreted the lowest part of the interval to represent gravelly bar sediments deposited in a low-sinuosity braided stream system during the early stage of regression across the eastern Kopet-Dagh basin. The middle part of the interval was deposited as a distal braidplain in an arid to semi-arid climate, with calcite nodules having formed as calcrete deposits. The upper part of the interval was deposited in a meandering stream system with fine-grained sediments recording floodplain deposition between episodes of meandering channel and point-bar deposition. The latest phase of deposition ended as

the sea transgressed northwestward across the Sarakhs area and marine sedimentation was established. The shallow-marine oolitic and skeletal calcarenites of the Tirgan Formation were then deposited through the remainder of the Neocomian and into the Aptian across the study area.

Correlations between the outcrop belt and the wells in the Sarakhs area (Figure 4) are based on the positions of units within a stratigraphic sequence between major unconformities, and by extrapolations made using depositional reconstructions and subsequently developed facies models (Moussavi-Harami and Brenner, 1990 and unpublished data). These models allow us to predict the distal facies distributions within the stratigraphic sequence northward from the outcrop belt, and then fit the lithofacies observed in the well cores of the sequence into the extrapolated facies. In this way, we can correlate the lower, middle, and upper parts of the Shurijeh Formation on the outcrop belt to their downdip corresponding facies in the cores from the KG-2, GL-2, and GL-3 wells. This procedure is similar to that discussed and illustrated by Brenner and McHargue (1988).

#### Postburial History of the Shurijeh Formation

Analyses of Shurijeh Formation specimens collected from both outcrop and subsurface sandstone samples show a specific sequence of diagenetic products formed by processes influenced by the succession of depositional environments and the burial history of the Kopet-Dagh basin (Moussavi-Harami and Brenner, unpublished data). These processes operated within two of the three hydrologic regimes defined by Galloway (1984): meteoric and compactional. Meteoric regime sediments are in contact with waters flowing down topographic gradients from surface recharge areas. The compactional regime is characterized by upward and outward expulsion of pore waters from compacting sediments. Early processes began in the meteoric regime and were controlled to a large extent by the aqueous chemistries present at the sites of deposition. Some of these processes continued into the compactional regime. Other processes were initiated as waters from deeper parts of the Kopet-Dagh basin were flushed through the Neocomian sandstones as they subsided within the compactional regime. Samples from outcrop sections show additional late features that resulted from renewed meteoric flushing during post-Miocene uplift and exposure.

The porous and permeable sand-rich units were cemented by infiltrated clays, early calcite, anhydrite, and silica as they subsided through the meteoric regime. In the compactional regime, feldspars altered to clays, dolomite replaced calcite and penetrated authigenic silica, and late-stage calcite cementation and replacement took place. These diagenetic events were

followed by partial dissolution of early and late-stage calcite cements that created secondary porosity in the sandstone units (Moussavi-Harami and Brenner, unpublished data). During the late Miocene–early Pliocene (approximately 10 Ma), the late Alpine orogeny affected the Kopet-Dagh basin, forming structural traps in the Shurijeh Formation of the Sarakhs area. At this time, gas migrated into the porous units of this formation, accounting for the Khangiran and Gonbadli gas fields.

#### Lithofacies and Reservoir Properties

In the Khangiran Gas field (KG-2 well), porous and permeable reservoir units are found in low-sinuosity, braided-stream-channel sandstone-conglomerate complexes in the lower part of the Shurijeh Formation. Primary porosity in these sandstones was destroyed early in their diagenetic histories, and gas accumulated in secondary pores formed by dissolution of calcite just prior to gas generation and migration (Moussavi-Harami and Brenner, unpublished data). The thin sheets of sandstone in the middle part of the Shurijeh lack gas accumulations due to their low original permeability and pervasive early cementation. The relatively “clean” fine-grained sandstones in the upper part of the Shurijeh lack significant porosities in the Khangiran field, probably because they were cemented within the meteoric regime and secondary porosity failed to develop prior to gas generation. However, in the Gonbadli field (GL-3 well), porous and permeable sandstones in the lower part of the upper part of this formation contain potentially economic gas accumulations. The upper part of this same interval consists of tightly cemented “clean” sandstone. Apparently, fluids released by the compacting sediment column were acidic enough to dissolve calcite cement in the lower sandstone units in this part of the Shurijeh, but were buffered by dissolved carbonate to the extent that they could not dissolve the cements of the upper sandstone units.

Figure 4 shows the distributions of porous and permeable intervals in the Khangiran and Gonbadli fields and the lack of communication between good reservoir intervals caused by intervening low-permeability fluvial-plain deposits.

#### Diagenetic Processes and Geohistory

The sequence of diagenetic processes that determined reservoir properties of Shurijeh sandstones was related to the burial history of the Kopet-Dagh basin. Figure 5A shows that the Shurijeh Formation had an uncompacted thickness of 352 m, and that these sediments subsided at a relatively high rate from the Neocomian to the late Eocene-early Oligocene (about 37

Ma). Figure 5B shows the paragenetic sequence of Neocomian Shurijeh sandstones plotted on the same temporal scale as in the geohistory diagram (Figure 5A). The beginning and end of each diagenetic process were approximated based on petrographic observations (Moussavi-Harami and Brenner, unpublished data). During the early meteoric phase of burial, these sandstones were subjected to detrital clay infiltration, compaction, calcite cementation, silica cementation, iron-oxide cementation, and anhydrite cementation, each of which contributed to the reduction of primary porosities from an average of 45% to nearly 0% in some units. Processes that operated in the compactional regime generally enhanced sandstone reservoir properties by creating secondary porosity. These processes included feldspar alteration to clay minerals, dolomitization of calcite, and calcite replacement of silica followed by calcite dissolution. These processes, along with late calcite cementation and penetration of authigenic silica by dolomite rhombs, preceded gas migration into these sandstones.

The hydrocarbon source rocks in this part of the Kopet-Dagh basin are believed to be the marlstones of the Middle Jurassic Chaman Bid Formation (Figure 2) (Afshar-Harb, 1979). According to the paleotemperature analysis of Afshar-Harb (1979), and the fact that gas traps were formed during the late Alpine orogeny, these Jurassic source rocks reached thermal maturity no earlier than the late Paleocene (about 50–60 Ma), and gas migration into the present structures took place no earlier than 10 Ma. Late Miocene uplift and erosion brought the Neocomian rocks along the present-day outcrop belt back into the meteoric regime. Iron-oxide formation and carbonate cement dissolution during the late meteoric phase of diagenetic alterations to the Shurijeh sandstones did not affect reservoir properties in the subsurface.

**CONCLUSIONS**

Geohistory diagrams for the eastern part of the Kopet-Dagh basin indicate that since the middle Early Cretaceous, the major factor that contributed to basin subsidence was sediment loading rather than tectonic subsidence. This observation shows how a relatively thick package of shallow-marine to terrestrial sediments could have accumulated in a basin that has undergone minimal tectonic subsidence. By combining sedimentologic, petrologic, and geohistory analyses, we have shown that reservoir properties of siliciclastic sandstones in the Lower Cretaceous (Neocomian) Shurijeh Formation in the eastern Kopet-Dagh basin in northeastern Iran vary according to their stratigraphic position in a sediment column, as well as to their original sedimentologic characteristics and pore fluid chemistry. "Clean" sands deposited in fluvial channel systems all started with high porosities and good

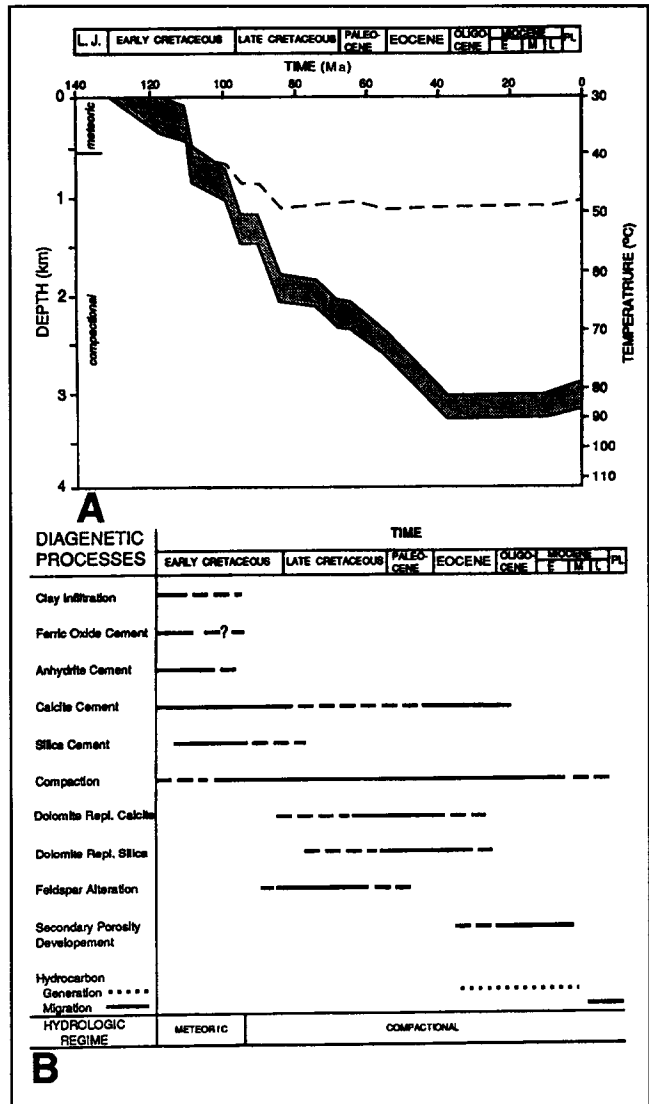


**Figure 5—Relationship between burial history of the Shurijeh Formation and paragenetic sequence observed in its sandstone units. (A) Geohistory diagram of the Shurijeh Formation (stippled pattern) in the eastern part of the Kopet-Dagh basin based primarily on data from the GL-3 well. Dashed line shows tectonic subsidence at base of the formation. Solid line at base of Shurijeh Formation represents total subsidence. Computation procedures are described in the text. (B) Paragenetic sequence for Shurijeh sandstones. Dashed line segments represent inferred ranges of diagenetic processes. Solid lines represent ranges interpreted from petrographic and geohistory relationships.**

permeabilities. They were invariably cemented within the meteoric regime resulting in nearly total destruction of primary porosities. Low-sinuosity, braided channel fills in the lower part of the Shurijeh Formation were subjected to acidic fluids generated in the compactional



regime, causing calcite cement dissolution and the formation of secondary porosity. These units provided reservoirs for gas that migrated into the Neocomian section in the Sarakhs area, resulting in the formation of the Khangiran gas field. At approximately the same time, high-sinuosity meander-channel fills in the lower part of the upper Shurijeh Formation underwent a similar diagenetic history. This resulted in the formation of reservoir units in the Gonbadli field.

Similar diagrams and analyses can be used in other parts of this and comparable basins to help develop models to predict the timing of such events as degradation of primary porosity and creation of secondary porosity, as well as hydrocarbon maturation, migration, and entrapment.

#### REFERENCES CITED

- Afshar-Harb, A., 1969, A brief history of geological exploration and geology of the Sarakhs area and the Khangiran gas field (in Persian): *Bulletin of the Iranian Petroleum Institute*, no. 37, p. 86–96.
- Afshar-Harb, A., 1979, The stratigraphy, tectonics and petroleum geology of Kopet-Dagh region, northern Iran: Ph.D. thesis, Petroleum Geology Section, Imperial College, London, 316 p.
- Afshar-Harb, A., 1982, Geological map of Sarakhs area: Ministry of Petroleum, NIOC Exploration and Production, Teheran, 1 sheet.
- Angevine, C. L., P. L. Heller, and C. Paola, 1990, Quantitative sedimentary basin modeling: AAPG Continuing Education Course Note Series #32, 133 p.
- Berberian, M., and G. C. P. King, 1981, Toward a paleogeography and tectonic evolution of Iran: *Canadian Journal Earth Sciences*, v. 18, p. 210–265.
- Brenner, R. L., and T. R. McHargue, 1988, Integrative stratigraphy—concepts and applications: Englewood Cliffs, New Jersey, Prentice Hall, 417 p.
- Galloway, W. E., 1984, Hydrogeologic regimes of sandstone diagenesis, in D. A. McDonald and R. C. Surdam, eds., *Clastic diagenesis: AAPG Memoir 37*, p. 2–13.
- Haq, B. U., J. Hardenbol, and P. R. Vail, 1987, Chronology of fluctuating sea levels since the Triassic: *Science*, v. 235, p. 1156–1167.
- Huber, H., 1975, Geological map of Iran, sheet no. 3, north-east Iran: NIOC Exploration and Production Affairs, Teheran, 1 sheet.
- Kalantari, A., 1969, Foraminifera from the Middle Jurassic–Cretaceous successions of Kopet-Dagh region (NE Iran): NIOC Geological Laboratories Publication no. 3, 298 p.
- Kalantari, A., 1987, Biofacies map of Kopet-Dagh region: Unpublished map, NIOC Exploration and Production, Teheran, 1 sheet.
- Madani, M., 1977, A study of the sedimentology, stratigraphy and regional geology of the Jurassic rocks of eastern Kopet-Dagh, NE Iran: Ph.D. thesis, Petroleum Geology Section, Imperial College, London, number of pages unknown.
- Moussavi-Harami, R., 1986, Neocomian (Lower Cretaceous) continental sedimentation in eastern Kopet-Dagh basin in NE Iran (abs.): 12th International Sedimentologic Congress, Canberra, Australia, p. 220.
- Moussavi-Harami, R., 1989, Depositional history of Upper Jurassic (Oxfordian–Kimmeridgian) carbonates and evaporites in north-eastern Iran (abs.): *Twenty-Eighth International Geological Congress Abstracts*, v. 2, p. 471.
- Moussavi-Harami, R., 1990, Lithostratigraphy and depositional history of the Upper Jurassic (Oxfordian–Kimmeridgian) rocks in Col-e-Malkabad area in southwest Aq-Darband (abstract in Persian): *Eighth Geological Symposium of Iran*, Geological Survey of Iran, p. 6–8.
- Moussavi-Harami, R., and R. L. Brenner, 1990, Lower Cretaceous (Neocomian) fluvial deposits in eastern Kopet-Dagh basin, north-eastern Iran: *Cretaceous Research*, v. 11, p. 163–174.
- Slater, J. G., and P. A. F. Christie, 1980, Continental stretching: an explanation of the post-mid-Cretaceous subsidence of the central North Sea Basin: *Journal of Geophysical Research*, v. 85, p. 3711–3739.
- Van Hinte, J. E., 1978, Geohistory analysis—application of micropaleontology in exploration geology: *AAPG Bulletin*, v. 62, p. 201–222.